IL NUOVO CIMENTO **39 C** (2016) 372
DOI 10.1393/ncc/i2016-16372-0

Colloquia: SEA2016

Cluster structure of neutron-rich ^{10}Be and ^{14}C via resonant alpha scattering

D. Suzuki(1), T. Ahn(2), D. Bazin(3), F. D. Becchetti(4), S. Beceiro-Novo(3), A. Fritsch(5), J. J. Kolata(2) and W. Mittig(3) for the AT-TPC Collaboration

(1) *RIKEN Nishina Center - Wako, Saitama, Japan*
(2) *Department of Physics, University of Notre Dame - Notre Dame, IN, USA*
(3) *National Superconducting Cyclotron Laboratory, Michigan State University East Lansing, MI, USA*
(4) *Department of Physics, Randall Laboratory, University of Michigan Ann Arbor, MI, USA*
(5) *Gonzaga University, Department of Physics - Spokane, WA, USA*

received 28 November 2016

Summary. — Neutron-rich ^{10}Be and ^{14}C nuclei were studied via resonant α scattering of radioactive ^{6}He and ^{10}Be beams, respectively, produced by the *TwinSol* facility at the University of Notre Dame. The Prototype Active-Target Time-Projection Chamber (pAT-TPC) was used as a thick gaseous α target to induce resonant scattering and as a device to track reacted particles inside the target, providing continuous excitation functions and angular distributions over a wide range of energies and angles. The experimental results indicate a melting phenomenon of α clusters in the 4^+ rotational member of the ^{10}Be ground state and a linear chain alignment of three α clusters in ^{14}C excited states, as recently predicted by an anti-symmetrized molecular dynamics calculation.

1. – Introduction

Studies of α clustering, dated back to as far as the 1930s [1], still constitute the forefront in modern nuclear physics. Neutron-rich nuclei have increasingly attracted attention in recent years. If clustering occurs, these nuclei represent a hybrid system, where excess neutrons around α clusters add another degree of freedom, prompting questions on whether α clusters in stable nuclei with equal numbers of protons (Z) and neutrons (N) persist as they are, or change their cluster properties such as geometrical alignment, or even dissolve into a shell-model-like state. Neutron-rich ^{10}Be and ^{14}C are very important nuclei to answer these questions since their $N = Z$ isotopes, ^{8}Be and ^{12}C, have arguably the best established cluster states, that are even reproduced by *ab initio* calculations using bare nuclear forces [2, 3]. Previous theoretical studies by the molecular orbital model [4], the anti-symmetrized molecular dynamics (AMD) approach [5-7], the multicluster generator coordinate method [8], and full [9, 10] or semi microscopic cluster models [11] show that the two valence neutrons of ^{10}Be and ^{14}C significantly impact the α clustering, predicting molecular neutron orbitals [4], or linear chain alignment of α clusters [7], the phenomenon that was first conjectured for the $N = Z$ nuclei [12], but remains unidentified even for the simplest 3α case in ^{12}C [13, 14]. While a number of experiments have been carried out [15-22], most of the predicted cluster states remain unknown or to be studied.

We studied ^{10}Be [23] and ^{14}C [24] via α resonant scattering off radioactive ^{6}He and ^{10}Be beams, respectively. The active target and time-projection chamber, Prototype AT-TPC (pAT-TPC) [25] containing He and CO_2 gas mixture was used as a reaction target as well as tracking medium of charged particles. The thick target method [26], where excitation functions are measured by decelerating beam particles over the length of a thick target, was used. Measuring reaction trajectories inside the target, commonly called active target technique [27], allows one to directly determine the reaction vertex and unambiguously deduce the beam energy, which translates into the resonance energy [23, 24, 28]. This would otherwise be limited with the widely-used multiple silicon detector setup that indirectly determines the reaction vertex, by assuming reaction kinematics energetically allowed, from the energy and angle of an α particle after leaving the target. The active target method enables the measurement of wide-ranging and continuous excitation functions and angular distributions, facilitating the identification of unknown resonances and oscillatory diffraction patterns, which are the most reliable information in determining the spin and parity.

2. – Experiment

These measurements were performed as the first series of experiments of the pAT-TPC using *TwinSol* [29] radioactive-ion beams at the FN tandem accelerator facility of the University of Notre Dame [30]. ^{6}He ions were produced via the $(d,{}^{3}\mathrm{He})$ reaction using a deuterium target at 1200 mm-Hg and 29.2 MeV ^{7}Li (3+) primary beam. To produce ^{10}Be ions, a stack of four 0.1 mg/cm^2 thick ^{13}C targets were bombarded by a 46 MeV ^{11}B(5+) primary beam. Radioactive ions thus produced were collected and purified in flight by the *TwinSol* device [29] consisting of a pair of solenoidal magnets. The secondary beam was delivered to the cylindrical target volume of He:CO_2 90:10 mixture gas at 1 atm of the pAT-TPC [25], measuring 50 cm along the beam axis and 27 cm in diameter. The beam energies of ^{6}He and ^{10}Be were 15 and 40 MeV, respectively. The corresponding center-of-mass energies $E_{\mathrm{c.m.}}$ (6 MeV for ^{6}He and 11.3 MeV for ^{10}Be) decreased to zero while travelling the length of the gas volume. The average rate of ^{6}He that entered the volume was 2×10^3 ions per second with a purity of 90%. The main impurity was ^{4}He. The average rate of ^{10}Be was 10^3 ions per second. The beam purity was about 35% with main contaminants of ^{4}He(2+) (50%), ^{9}Be(4+) (5%), and ^{10}B(4+) (3%). Electrons from reaction trajectories are guided toward the Micromegas amplifier [31] by an electric field of 0.8 kV/cm parallel to the beam axis. The Micromegas consists of 2 mm wide radial strips separated into quadrants. A waveform digitizer [32] records the charge as a function of drift time over 40 μs by using an array of 511 switching capacitors.

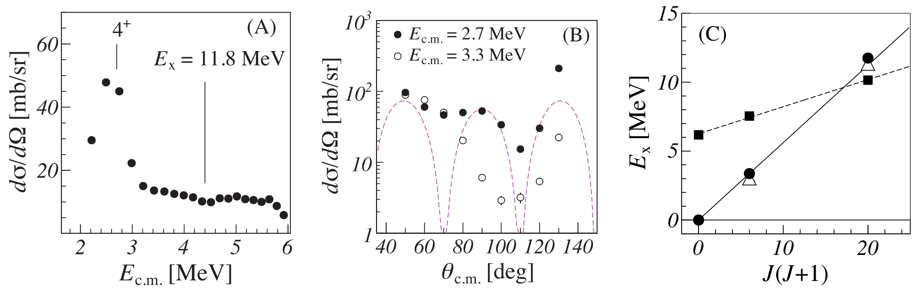

Fig. 1. – (A) Excitation function for ^{6}He + α elastic scattering. The data are integrated over $\theta_{\mathrm{c.m.}} = 65°$–$135°$. The observed 4^+ resonance at around $E_{\mathrm{c.m.}} = 2.7\,\mathrm{MeV}$ and the missing 4^+ resonance expected from a ^{10}Be state at $E_{\mathrm{x}} = 11.8\,\mathrm{MeV}$ are denoted by the lines. (B) Differential cross sections of ^{6}He + α elastic scattering for the 4^+ resonance at $E_{\mathrm{c.m.}} = 2.7\,\mathrm{MeV}$ (filled circles). Off-resonance data at 3.3 MeV (open circles) are also shown for reference. The oscillatory pattern of the 2.7 MeV data agrees with that of the squared Legendre function with $L = 4$ (dashed line), for which an arbitrary scaling factor was adopted for presentation purposes. (C) Excitation energies *vs.* $J(J+1)$ plot for rotational band members of the ground (circles) and second (squares) 0^+ states of ^{10}Be. The ground-state band members of ^{8}Be (triangles) are also shown for comparison.

3. – Results

The angle-integrated excitation function for ^{6}He elastic scattering is shown in fig. 1(A). While elastic scattering was previously measured at several beam energies [15-17, 19], this is the first differential cross section data taken continuously over a finite range of energy. The resonance visible at $E_{\mathrm{c.m.}} = 2.56(15)\,\mathrm{MeV}$ is assigned a spin and parity of 4^+ from the diffraction seen in the angular distribution of fig. 1(B), which excellently agrees with the oscillatory pattern of the squared Legendre function for an angular momentum $L = 4$. The partial α decay width was estimated to be $\Gamma_\alpha/\Gamma = 0.49(5)$ from the resonance cross sections. These results are in line with the previous measurement with a narrower energy range, but with better statistics [19]. The large partial width of this 4^+ state, widely considered as the 4^+ member of the second 0^+ rotational band, supports the predicted σ-type molecular orbital structure around the two α clusters [4, 5]. Another 4^+ state of the ground state 0^+ band, often discussed as a π-type partner of the second 0^+ band, is predicted at $E_{\mathrm{c.m.}} = 3$ to 6 MeV by several calculations [4-6, 8, 10, 11]. This state has been associated with a ^{10}Be level found at an excitation energy (E_{x}) of 11.76 MeV [20], or $E_{\mathrm{c.m.}} = 4.36\,\mathrm{MeV}$, given the α emission threshold at $E_{\mathrm{x}} = 7.4\,\mathrm{MeV}$. However, our result that allowed us to survey a wide range of excitation energies up to $E_{\mathrm{c.m.}} = 6\,\mathrm{MeV}$ rules out resonances at predicted energies, with an upper limit of $\Gamma_\alpha = 20\,\mathrm{keV}$. This is almost one order of magnitude small than that of the 2.56 MeV resonance with $\Gamma_\alpha = 145(15)\,\mathrm{keV}$. The missing resonance strength and the hindered branching for α emission indicate that the degree of clusterization is reduced in the 4^+ state of the ground state 0^+ rotational band. The weakening of clustering is pointed out by an early AMD study of ^{10}Be [5], predicting that the α clusters in the 0^+ ground state gradually dissolve in the rotational band members as the total spin increases. It is interesting to note that the ground state band of ^{10}Be has almost the same level spacing as ^{8}Be (fig. 1(C)), while the α clustering in ^{8}Be appears to be robust in 0^+, 2^+, and 4^+ states. The α spectroscopic factors of ^{8}Be are equally large in all of

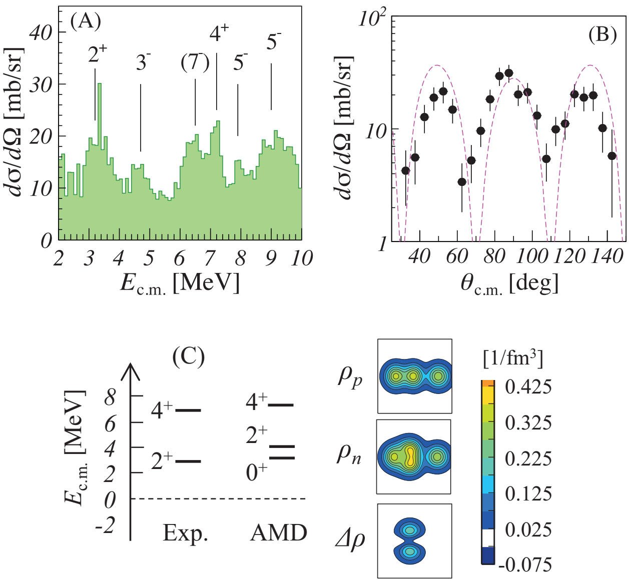

Fig. 2. – (A) Excitation function for ^{10}Be + α elastic scattering. Resonances of ^{14}C and their spins and parities from the present analysis are shown. (B) Differential cross sections of ^{10}Be + α elastic scattering for the resonance at $E_{\mathrm{c.m.}} = 7.0\,\mathrm{MeV}$ (filled circles). The oscillatory pattern agrees with that of the squared Legendre function with $L = 4$ (dashed line), for which an arbitrary scaling factor was used. (C) Comparison of the 2^+ and 4^+ resonance energies to the linear 3α chain states predicted in a β-γ constraint AMD study [7]. The proton (ρ_p) and neutron (ρ_n) density distributions and their differential ($\Delta\rho = \rho_p - \rho_n$) for the predicted linear chain states are displayed.

these states according to the folding-model potential calculation that well describes the level energies and widths of these states [33]. In one *ab initio* Quantum Monte Carlo calculation of ^{8}Be [2], the density distribution of the 4^+ state shows the two α clusters as clearly as in the 0^+ ground state. The dissociation of α clusters in ^{10}Be, which thus stands in stark contrast with ^{8}Be, may be due to the two excess neutrons that complete the filling of the $1p_{3/2}$ orbital. The large energy gap relative to the higher $1p_{1/2}$ orbital that gives rise to the subshell closure at $N = 6$ may favour shell-model-like structure over the α clustering.

The excitation function for elastic α scattering of ^{10}Be is shown in fig. 2(A). Among several resonances of ^{14}C identified, there are two positive-parity states, one being a 2^+ state at $E_{\mathrm{c.m.}} = 3.0\,\mathrm{MeV}$, the other a 4^+ state at $7.0\,\mathrm{MeV}$. These spin and parity assignments were made again from the oscillation patterns of differential cross sections (fig. 2(B)). These levels are compared to a β-γ constraint AMD calculation using the generator coordinator method [7] in fig. 2(C). The experimental resonance energies well agree with the 2^+ and 4^+ states of one of the rotational bands predicted. As seen in the intrinsic density distributions, three α clusters are aligned in a linear arrangement in this band. This supports the presence of a linear 3α chain structure in excited states of ^{14}C.

4. – Summary

To study the cluster structure of ^{10}Be and ^{14}C, resonant α scattering of radioactive ^{6}He and ^{10}Be beams was measured at the *TwinSol* facility using the pAT-TPC. The hindered branching for α emission observed for the 4^+ rotational member of the ^{10}Be ground state indicates that the α clustering of the ground state, consistently predicted by different theoretical studies, fades away in the 4^+ rotational member. The newly-found 2^+ and 4^+ states of ^{14}C agree with linear chain states predicted by the recent AMD work. The α clustering is robust against dissociation in ^{8}Be and the linear chain structure is predicted to be manifested very weakly in ^{12}C. The present results suggesting these phenomena realized in ^{10}Be and ^{14}C indicate that two valence neutrons alone can drastically and essentially evolve the α cluster structure.

* * *

This work was supported by the National Science Foundation under Grant Nos. PHY09-69456, PHY14-01343, PHY14-19765, PHY14-30152, and MRI09-23087.

REFERENCES

[1] Wheeler J. A., *Phys. Rev.*, **52** (1937) 1083.
[2] Wiringa R. B., *Phys. Rev. C*, **62** (2000) 014001.
[3] Epelbaum E. *et al.*, *Phys. Rev. Lett.*, **109** (2012) 252501.
[4] Itagaki N. and Okabe S., *Phys. Rev. C*, **61** (2000) 044306.
[5] Kanada-En'yo Y. *et al.*, *Phys. Rev. C*, **60** (1999) 064304.
[6] Suhara T. and Kanada-En'yo Y., *Prog. Theor. Phys.*, **123** (2010) 303.
[7] Suhara T. and Kanada-En'yo Y., *Phys. Rev. C*, **82** (2010) 044301.
[8] Descouvemont P., *Nucl. Phys. A*, **699** (2002) 463.
[9] Ito M. *et al.*, *Phys. Lett. B*, **588** (2004) 43.
[10] Hernández de la Peña L. *et al.*, *J. Phys. G*, **27** (2001) 2019.
[11] Arai K., *Phys. Rev. C*, **69** (2004) 014309.
[12] Morinaga H., *Phys. Rev.*, **101** (1956) 254.
[13] Neff T. and Feldmeier H., *Nucl. Phys. A*, **738** (2004) 357.
[14] Suhara T. and Kanada-En'yo Y., *Prog. Theor. Phys.*, **123** (2010) 303.
[15] Ter-Akopian G. M. *et al.*, *Phys. Lett. B*, **426** (1998) 251.
[16] Raabe R. *et al.*, *Phys. Lett. B*, **458** (1999) 1.
[17] Raabe R. *et al.*, *Phys. Rev. C*, **67** (2003) 044602.
[18] von Oertzen W. *et al.*, *Eur. Phys. J. A*, **21** (2004) 193.
[19] Freer M. *et al.*, *Phys. Rev. Lett.*, **96** (2006) 042501.
[20] Bohlen H. G. *et al.*, *Phys. Rev. C*, **75** (2007) 054604.
[21] Haigh P. J. *et al.*, *Phys. Rev. C*, **78** (2008) 014319.
[22] Freer M. *et al.*, *Phys. Rev. C*, **90** (2014) 054324.
[23] Suzuki D. *et al.*, *Phys. Rev. C*, **87** (2013) 054301.
[24] Fritsch A. *et al.*, *Phys. Rev. C*, **93** (2016) 014321.
[25] Suzuki D. *et al.*, *Nucl. Instrum. Methods Phys. Res. A*, **691** (2012) 39.
[26] Artemov K. P. *et al.*, *Sov. J. Nucl. Phys.*, **55** (1992) 1460.
[27] Beceiro-Novo S. *et al.*, *Prog. Part. Nucl. Phys.*, **84** (2015) 124.
[28] Sambi S. *et al.*, *Eur. Phys. J. A*, **51** (2015) 25.
[29] Becchetti F. *et al.*, *Nucl. Instrum. Methods Phys. Res. A*, **505** (2003) 377.
[30] Ahn T. *et al.*, *Nucl. Instrum. Methods Phys. Res. B*, **376** (2016) 321.
[31] Giomataris Y. *et al.*, *Nucl. Instrum. Methods Phys. Res. A*, **376** (1996) 29.
[32] Baron P. *et al.*, *IEEE Trans. Nucl. Sci.*, **NS-55** (2008) 1744.
[33] Mohr P. *et al.*, *Z. Phys. A*, **349** (1994) 339.